Environmental Science & Technology

Article

pubs.acs.org/est

Insights into Mechanistic Models for Evaporation of Organic Liquids in the Environment Obtained by Position-Specific Carbon Isotope Analysis

Maxime Julien,[†] Pierrick Nun,[†] Richard J. Robins,[†] Gérald S. Remaud,[†] Julien Parinet,[‡] and Patrick Höhener*[,‡]

[†]EBSI Team, CEISAM, University of Nantes−CNRS UMR 6230, 2 rue de la Houssinière BP 92208, F-44322 Nantes, France

[‡]Laboratoire Chimie Environnement, University of Aix-Marseille−CNRS FRE 3416, place Victor Hugo 3, F-13331 Marseille, France

Supporting Information

ABSTRACT: Position-specific isotope effects (PSIEs) have been measured by isotope ratio monitoring ^{13}C nuclear magnetic resonance spectrometry during the evaporation of 10 liquids of different polarities under 4 evaporation modes (passive evaporation, air-vented evaporation, low pressure evaporation, distillation). The observed effects are used to assess the validity of the Craig−Gordon isotope model for organic liquids. For seven liquids the overall isotope effect (IE) includes a vapor−liquid contribution that is strongly position-specific in polar compounds but less so in apolar compounds and a diffusive IE that is not position-specific, except in the alcohols, ethanol and propan-1-ol. The diffusive IE is diminished under forced evaporation. The position-specific isotope pattern created by liquid−vapor IEs is manifest in five liquids, which have an air-side limitation for volatilization. For the alcohols, undefined processes in the liquid phase create additional PSIEs. Three other liquids with limitations on the liquid side have a lower, highly position-specific, bulk diffusive IE. It is concluded that evaporation of organic pollutants creates unique position-specific isotope patterns that may be used to assess the progress of remediation or natural attenuation of pollution and that the Craig−Gordon isotope model is valid for the volatilization of nonpolar organic liquids with air-side limitation of the volatilization rate.

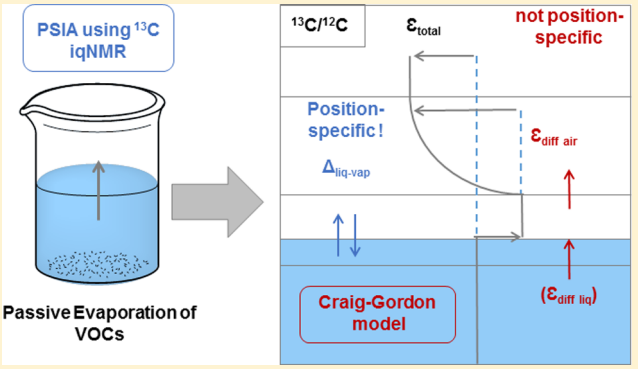

INTRODUCTION

Organic liquids such as solvents, fuels, and fuel additives are among the most problematic groundwater contaminants because they migrate actively to groundwater and form long-lasting sources. At many contaminated sites, extraction of compounds based on soil vapor, dual-phase extraction, or air-sparging is the chosen remediation strategy. Compound-specific isotope analysis (CSIA) can be a tool for the assessment of remediation success and is applied frequently for degradation processes involving strongly isotope-fractionating bond-breaking reactions.[1] However, diffusive isotope fractionation during volatilization can also create isotope fractionation, thus CSIA for remediation assessment is only possible when the mechanisms of volatilization are well understood and the pertinent isotope fractionation factors are quantified.[1] The earliest and most complete understanding of isotope fractionation during evaporation of a liquid is that for water and its isotopes ^{2}H and ^{18}O.[2−4] The well-accepted model of Craig and Gordon (CG-model) states that two isotope effects (IE)—the vapor−liquid IE and the diffusive IE—are implied in water evaporation and that the effects are additive. Vapor−liquid IEs for organic liquids were studied in the past by distillation and manometric methods[5] and, mostly, inverse carbon IEs were found for hydrocarbons (i.e., the vapors were enriched in ^{13}C compared to the liquids).[6−9] Harrington and co-workers,[10] who observed inverse IEs in aromatic hydrocarbons over a temperature range of 5−70 °C, suggested that the remaining contaminants would therefore become depleted in ^{13}C during volatilization. Bouchard and co-workers[11] found that the opposite is true for hydrocarbons evaporating from a mass of hydrocarbons buried in soil. This was interpreted as being the result of two IEs, of which the normal diffusive IE dominates over the inverse vapor−liquid IE for ^{13}C.[12] Kuder et al.[13] were the first to apply the CG-model to ^{2}H and ^{13}C IEs of passive and vented evaporation of an organic liquid pollutant, methyl *tert*-butyl ether (MTBE) . In contrast, Jeannottat and Hunkeler[14] used another model derived from the water evaporation model from He and Smith[3] to interpret results of ^{13}C and ^{37}Cl isotope measurements in TCE during

Received: July 7, 2015
Revised: September 29, 2015
Accepted: October 6, 2015
Published: October 6, 2015

DOI: 10.1021/acs.est.5b03280
Environ. Sci. Technol. 2015, 49, 12782−12788

evaporation through soil or in a fume hood. They found that the vapor−liquid IE and the diffusion IE for ^{13}C are of the same magnitude, but are of opposite direction, and thus, the overall effect is nil. Only for chlorine could an isotope fractionation be evaluated.[14]

A number of other studies measured carbon isotope fractionation of organic liquids during volatilization in fume hoods,[15−17] and fractionation was often quite different from what has been measured and predicted during volatilization from soil. The magnitude of airflow and the way by which the vapor is carried away seem to play a role, but no quantitative understanding for this is available.

Position-specific isotope analysis (PSIA) using isotope ratio monitoring by ^{13}C NMR (irm-^{13}C NMR) spectrometry is a powerful new tool to look at processes where CSIA by isotope ratio monitoring mass spectrometry (irm-MS) may not detect any effect on the whole molecule. In the current case, in which there are two additive processes, it can be anticipated that the vapor−liquid IE might be fairly position-specific, especially in liquids with polar interactions (e.g., where hydrogen bonding is occurring). In contrast, the IE for diffusion in gas phase should, a priori, not be position-specific. Thus, our working hypothesis is that by using PSIA, it is possible to assess progressive evaporation even for compounds where the bulk (or overall average for the compound) IE is nil, and gain new insights in the molecular understanding of the evaporation process. In a previous study,[18] we showed how irm-^{13}C NMR gives access to the position-specific isotope fractionation (PSIF), expressed as $\delta^{13}C_i$ and that the PSIF values may vary more significantly than the bulk $\delta^{13}C_b$ obtained by irm-MS.

In that former study, evaporation conditions on model molecules known as important pollutants (TCE, MTBE, toluene), and ethanol covered four processes: passive evaporation (PE), air-flux assisted evaporation (AFE), low pressure evaporation (LPE) and distillation (DE), and the $\delta^{13}C_i$ values were determined by irm-^{13}C NMR, with the objective to give a proof-of-concept for the use of PSIA in pollution studies.[18]

The objective of the present work is to probe the mechanisms underlying the changes in PSIEs during volatilization. For this, we have added 6 more compounds with significantly different chemical properties in terms of their polarity, volatility and liquid density: acetone, bromoethane, propan-1-ol, methanol, *n*-heptane, and *tert*-amyl methyl ether (TAME). These compounds were evaporated under the same evaporation modes as the four previous compounds.[18]

THEORY

Volatilization of liquids to the open air is best represented by a conceptual model based on two stagnant films, a liquid film on the liquid side and a gas film on the air side of the interface (Figure 1).[19] According to the physical conditions, either one of these films is the bottleneck for defining the overall flux rate, or both films may contribute to limit the speed of volatilization.

The outcome of the overall limitation depends on in which film the transfer velocity is smaller. Discussing IEs during volatilization thus requires the analysis of the transfer velocities in these films. For the evaporation of water, it is the air film which controls the overall flux rate.[2] For this situation, the CG-model was developed for ^{2}H and ^{18}O. It was later adopted by Kuder et al.[13] for describing the volatilization of MTBE from water when the flux limitation is also on the air side. The IE is composite, including two processes: the liquid−vapor IE

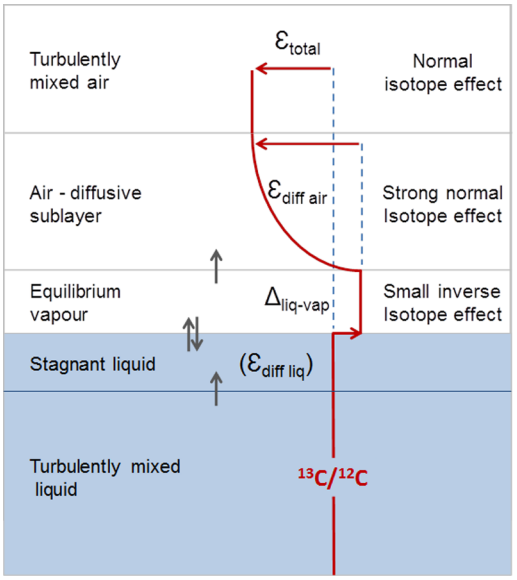

Figure 1. Schematic representation of the two-film model for isotope effects of a liquid undergoing volatilization with rate limitation on the air-side boundary.

($\Delta_{liquid-vap.}$), and the diffusion effect in the air film $\varepsilon_{diff\text{-}air}$. These effects are additive (eq 1):[13]

$$IE = \Delta_{liquid-vap} + \varepsilon_{diff-air} \text{ for air - film limited evaporation} \quad (1)$$

Liquid−vapor IEs ($\Delta_{liquid-vap}$) have been quite extensively studied in the classical isotope literature by distillation or manometric methods at different temperatures. Most organic liquids have inverse liquid−vapor carbon IE.[6] These IE are a result of higher dispersion (London) forces and hence higher densities and higher collision probability of compounds with a heavy isotope in the condensed phase. The IE is highly dependent on the position of the isotopic substitution: the liquid−vapor IE of *n*-octanols deuteriated on the OH group was strongest when the group was at the terminal position, and weakest when it was at one of the inner positions.[20] Further position-specific IEs were documented for other deuterated alcohols, acetic acid and toluene.[5] PSIEs were also observed for ^{13}C in ethanol in experiments based on distillation.[21]

The second process creating IEs in passive volatilization is the diffusion effect in the air film. This process is also well-known and is determined by mass difference between the isotopomers or isotopologues. Craig derived the fractionation factor for the diffusion effect in the air film $\alpha_{diff\text{-}air}$ (eq 2):[22]

$$\alpha_{diff\text{-}air} = \sqrt{\frac{M_l(M_h + M_{av})}{M_h(M_l + M_{av})}} \quad (2)$$

where M is molecular mass, and subscripts l, h, and av denote light or heavy isotopomers and air with compound vapor, respectively. The diffusion effect is not supposed to be position-specific and is always normal. For the molecular mass of air, 28.8 g mol^{-1} is often adopted, accounting for 20% O_2 and 80% N_2 in air. In the case of very volatile organic liquids, this value needs to be adjusted because the compound vapor can also account for some percentage of total air molecules. This is explained in more detail in the Supporting Information. The M_{av} values for the compounds in this study were calculated and are given in Table S3. Using this fractionation factor, and

DOI: 10.1021/acs.est.5b03280
Environ. Sci. Technol. 2015, 49, 12782−12788

Table 1. Bulk and Position-Specific Enrichment Factors Obtained for the Four Evaporation Modes and for the 10 Compounds Investigated[a]

			bulk		C-1		C-2		C-3		C-4		C-5	
compound	evaporation mode	f (%)	$\Delta\delta^{13}C_b$ (‰)	ε_b (‰)	$\Delta\delta^{13}C_i$ (‰)	ε_i (‰)	$\Delta\delta^{13}C_i$ (‰)	ε_i (‰)	$\Delta\delta^{13}C_i$ (‰)	ε_i (‰)	$\Delta\delta^{13}C_i$ (‰)	ε_i (‰)	$\Delta\delta^{13}C_i$ (‰)	ε_i (‰)
methanol	PE	4.8	+19.0	−6.5										
	AFE	7.3	+10.8	−4.2										
	LPE	4.0	−1.0	+0.3										
	DE	1.6	−2.1	+0.5										
ethanol	PE	7.3	+11.4	−4.3	+6.8	−2.6	+16.1	−6.1						
	AFE	7.3	+6.7	−2.5	+4.4	−1.7	+8.9	−3.3						
	LPE	4.0	−1.0	+0.4	−2.0	+0.7	+0.0	−0.0						
	DE	6.7	−1.8	+0.7	−2.9	+1.1	−0.7	+0.3						
acetone	PE	5.0	+7.3	−2.5	+4.0	−1.3	+8.9	−3.1						
	AFE	4.7	+7.0	−2.3	+3.8	−1.2	+8.5	−2.9						
	LPE	3.3	+1.0	−0.3	−1.1	+0.3	+2.0	−0.6						
	DE	3.0	+1.2	−0.3	−1.5	+0.4	+2.5	−0.7						
propan-1-ol	PE	6.4	+6.0	−2.3	+2.7	−1.0	+5.9	−2.2	+9.4	−3.5				
	AFE	5.2	+2.2	−0.8	+0.9	−0.3	+2.0	−0.7	+3.6	−1.2				
	LPE	7.0	−2.0	+0.8	−2.7	+1.1	−1.7	+0.7	−1.6	+0.6				
	DE	3.1	−3.1	+0.9	−3.6	+1.1	−3.1	+0.9	−2.5	+0.7				
MTBE	PE	6.0	+2.8	−1.0	+1.0	−0.4	+3.2	−1.2	+3.3	−1.2				
	AFE	5.0	+2.1	−0.7	+0.7	−0.2	+1.5	−0.5	+2.8	−1.0				
	LPE	4.3	+0.1	−0.0	−0.7	+0.2	+0.1	−0.0	+0.4	−0.1				
	DE	1.8	−1.3	+0.3	−4.1	+1.0	−0.8	+0.2	−0.6	+0.1				
toluene	PE	4.9	+2.8	−0.9	+0.9	−0.3	+2.5	−0.8	+2.6	−0.9	+2.8	−1.0	+5.4	−1.8
	AFE	3.1	+2.2	−0.6	+0.9	−0.2	+2.3	−0.7	+2.2	−0.6	+2.4	−0.7	+3.2	−0.9
	LPE	5.3	−0.8	+0.3	−2.1	+0.7	−0.9	+0.3	−0.7	+0.2	−0.4	+0.1	−0.1	+0.0
	DE	4.9	−1.4	+0.4	−0.8	+0.3	−1.4	+0.5	−1.5	+0.5	−2.3	+0.7	−0.8	+0.3
n-heptane	PE	6.1	+1.5	−0.5	+0.6	−0.2	+1.0	−0.4	+1.3	−0.5	+2.8	−1.0		
	AFE	5.1	+2.1	−0.7	+1.6	−0.5	+1.3	−0.5	+2.2	−0.8	+3.0	−1.0		
	LPE	3.7	−1.2	+0.4	−1.4	+0.4	−1.1	+0.4	−1.4	+0.4	−0.9	+0.3		
	DE	6.0	−1.9	+0.7	−2.2	+0.8	−1.2	+0.4	−2.0	+0.7	−1.8	+0.7		
TAME	PE	7.0	−0.1	+0.0	−2.1	+0.8	+1.0	−0.4	−0.2	+0.1	+0.5	−0.2	−0.5	+0.2
	AFE	6.2	+0.8	−0.3	−0.9	+0.3	+1.2	−0.5	+1.0	−0.4	+1.6	−0.6	+0.4	−0.2
	LPE	5.0	−0.6	+0.2	−1.6	+0.6	−0.3	+0.1	−0.7	+0.2	−0.2	+0.1	−0.8	+0.3
	DE	5.5	−1.7	+0.6	−3.2	+1.1	−0.6	+0.2	−1.9	+0.7	−1.4	+0.5	−1.9	+0.7
bromoethane	PE	6.4	−0.4	+0.2	−2.7	+1.0	+1.9	−0.7						
	AFE	5.2	+0.7	−0.2	−0.2	+0.1	+1.6	−0.6						
	LPE	5.6	−2.2	+0.8	−4.7	+1.7	+0.6	−0.2						
	DE	1.9	−2.8	+0.7	−4.3	+1.1	−1.4	+0.4						
TCE	PE	6.5	−1.1	+0.4	−2.1	+0.8	−0.1	+0.0						
	AFE	7.1	−0.6	+0.2	−1.3	+0.5	+0.0	−0.0						
	LPE	7.2	−1.4	+0.5	−1.5	+0.6	−1.3	+0.5						
	DE	4.7	−2.4	+0.8	−3.0	+1.0	−1.8	+0.6						

[a]Example calculation for isotope mass balance in compound MTBE: $\varepsilon_{bulk} = (\varepsilon_{C\text{-}1} + \varepsilon_{C\text{-}2} + 3x\ \varepsilon_{C\text{-}3})/5$

correcting for humidity and strength of airflow, the enrichment factor for diffusion in the air film is obtained (eq 3)[4]

$$\varepsilon_{diff\text{-}air} = n(1 - h)(\alpha_{diff\text{-}air} - 1) \times 1000 \quad (3)$$

where n is a factor used in the CG-model correcting for airflow (ranging from 1 in the absence of airflow to 0.5 in very turbulent airflow), and h is humidity in the case of water, or relative vapor saturation for organic compounds. eq 3 states that the diffusive IE disappears under very strong airflows or at 100% vapor saturation. Note that eq 3 is valid only for well-mixed liquids (i.e., for shallow pools).[2]

Kuder et al.[13] worked on the volatilization of pollutants from gasoline and calculated for a number of nonaqueous liquids whether the bottleneck for volatilization is in the air phase or on the liquid side. For pure organic liquids, a simplified way to answer this question is to calculate the air-organic liquid partitioning coefficient K_{ial} (Table S4). If this coefficient is $\ll 10^{-3}$ (Figure S2), then the limitation is on the air side.[19] The calculations suggest that for methanol, ethanol, propan-1-ol, toluene, *n*-heptane, TAME and TCE, the limitation is at the air side boundary, whereas for the 3 other compounds, either both boundaries or only the liquid side might limit the diffusive flux since K_{ial} is 10^{-3} or larger. By calculation, Kuder et al.[13] deduced air-side limitation for benzene, phenol, *p*-xylene, TCE and naphthalene, and about equal film limitation for MTBE, although it must be noted here that the method of calculation used by Kuder et al.[13] was specifically chosen for volatilization from gasoline and it involved *n*-octanol−water and air−water partitioning. The IE for volatilization in liquids limited on the liquid side would be according to (eq 4)[13]

DOI: 10.1021/acs.est.5b03280
Environ. Sci. Technol. 2015, 49, 12782−12788

$$\mathrm{IE} = \varepsilon_{\mathrm{diff-liquid}} \text{for liquid film} - \text{limited evaporation} \quad (4)$$

with $\varepsilon_{\mathrm{diff\text{-}liquid}}$ being the isotope enrichment due to diffusion in the liquid phase. Note that here no liquid−vapor IE applies, and neither airflow nor vapor saturation should have any influence on the IE. It is clearly smaller in magnitude than the diffusion effect in air.

The fractionation by diffusion in liquid phase was assumed to be approximately equal to the square root of the inverse ratio of the molar masses based on the Stokes−Einstein equation.[23,24] Recent work of diffusion of TCE[25] or noble gases[26] in water revealed that this method overestimates diffusive fractionation, and that molecular dynamics simulations[24] give a better insight into the magnitude of fractionation.

EXPERIMENTAL SECTION

Chemicals and Evaporation Experiments. The sources and quality of the evaporated chemicals and their physicochemical characteristics are given in the Supporting Information. The evaporation simulation was performed from four different experiments using 20 or 100 mL of pure compound: the remaining substrate (2−7%) was submitted to isotope analysis. The "passive" evaporation (PE) was carried out with 20 mL of compound in a 30 mL vial under fume-hood at constant airflow of 2×10^5 L h^{-1} at an ambient temperature of approximately 22 °C. The "air flux" evaporation (AFE) was performed with 20 mL of pure chemicals in a 250 mL three-necked round-bottom flask with two open necks and the third connected to an inlet blowing air at 500 L h^{-1}. Evaporation at "low-pressure" (LPE) was done on 20 mL compound, using a Rotavapor with a 30 °C water bath and a vacuum of about 10 mbar. Evaporation upon distillation (DE) was carried out using a spinning band (Cadiot) distillation column[8] on 100 mL of each compound.

Isotope Ratio Monitoring ^{13}C NMR Spectrometry (irm-^{13}C NMR). The protocols for sample analysis were described previously.[18] Only a brief summary is given here, and more details are supplied in the Supporting Information (Tables S1 + 2). Quantitative ^{13}C NMR spectra were recorded using a Bruker AVANCE I 400, fitted with a 5 mm i.d. ^{1}H/^{13}C dual$^+$ probe, carefully tuned at the recording frequency of 100.61 MHz, or a Bruker AVANCE III fitted with a 5 mm i.d. BBFO probe tuned at the recording frequency of 100.62 MHz. In all cases the temperature of the probe was set to 303 K. The offset for ^{13}C frequencies was set at the middle of the frequency range observed for each studied compound. An inverse-gated decoupling technique has been used to avoid Nuclear Overhauser Effect (NOE).

Isotope ^{13}C/^{12}C ratios were calculated from processed spectra essentially as described previously.[27,28] The isotope enrichment fractionation factor ε was calculated according to the common Rayleigh approach (equation S2, Supporting Information).

Isotope Ratio Monitoring MS (irm-MS). Bulk ^{13}C abundance ($\delta^{13}C_b$) was determined by isotope ratio monitoring mass spectrometry (irm-MS) using an Integra2 spectrometer (Sercon Instruments, Crewe, UK) linked to an elemental analyzer (irm-EA/MS) (Sercon Instruments, Crewe, UK). A precise mass of compound was weighted into tin capsules (2 × 5 mm, Thermo Fisher Scientific) using a 10^{-6} g precision balance (Ohaus Discovery DV215CD) to have ∼0.4 mg of carbon/capsule. Precautions were taken to ensure the quality of sealing of the capsules to avoid leakage. δ^{13}C (‰) values are expressed relative to the international reference (Vienna-Pee Dee Belemnite, V-PDB) using the relation:

$$\delta^{13}C\ (‰) = \left(\frac{R_{\mathrm{sample}}}{R_{\mathrm{reference}}} - 1\right) \times 1000 \quad (5)$$

Calibrated of δ^{13}C was via a laboratory standard of glutamic acid standardized against calibrated international reference materials (NBS-22, IAEA-CH-6, IAEA-CH-7).

RESULTS

Bulk ^{13}C Fractionation upon Evaporation Simulations. Table 1 shows bulk enrichment factors obtained in this study for the four evaporation modes and for the 10 compounds investigated. The compounds are ordered with respect to increasing molar mass and the numbering of the carbon atoms, as depicted in Figure 2, is from the low field to the high field in the ^{13}C NMR spectra. For DE, all enrichment factors except for acetone are positive, meaning that the IEs are inverse except for acetone. In contrast, for PE and AFE, IEs are inverse only for the two halogenated compounds, whereas all eight other compounds exert significant normal IEs. When the calculated bulk IEs are compared to values published in the literature, a good agreement is generally found for all DE values, and a poorer agreement for passive volatilization (Supporting Information, Table S6).

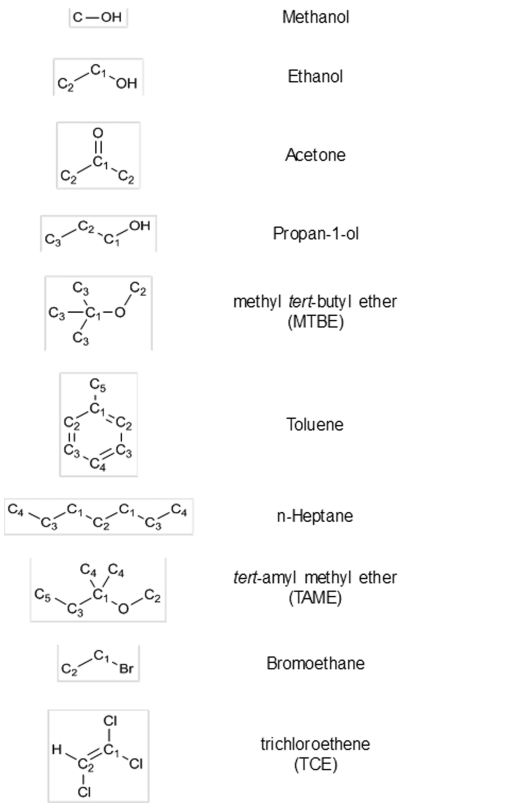

Figure 2. Numbering of positions according to the shielding order of the peak appearance on the ^{13}C NMR spectra.

Position-Specific^{13}C Fractionation upon Evaporation Simulations. Figure 2 shows the numbering of positions according to the shielding order of the peak appearance on the ^{13}C NMR spectra.

DOI: 10.1021/acs.est.5b03280
Environ. Sci. Technol. 2015, 49, 12782−12788

From the $\delta^{13}C_i$ values determined by irm-^{13}C NMR, the enrichment factor ε_i was calculated as shown in the Supporting Information. As discussed previously,[12] the uncertainty of ε_i is ±0.2‰, as calculated from the GUM guide.[29] The results reveal that PSIEs are occurring in all compounds that have more than one isotopomer, and that most frequently the carbon at position 1 is subject to the largest inverse IE (or the lowest normal IE). Intramolecular variation of enrichment is sometimes not very large and may be smaller than analytical uncertainty, as in the apolar compound *n*-heptane, the weakly monopolar compound toluene, and even in the monopolar compounds, TAME and TCE, but remains significant. Stronger intramolecular variations are demonstrated in the polar compounds, ethanol, propan-1-ol, MTBE, bromoethane, and acetone. Strong intramolecular variations are manifested in all evaporation modes except LPE. This latter mode produces in general the smallest bulk IE and PSIE. It is noteworthy here that the pattern of intramolecular variation is equal in the three strongly differentiating modes. For example, in the case of MTBE, the enrichment factor at C-1 is always larger than those for C-2 and C-3. The PE and the DE ε_i values show similar distribution of the IE in the molecule at different absolute magnitude.

DISCUSSION

Following the theory developed in the Theory section and the evaporation modes applied in this study, it is assumed that the following IEs will be active. (1) In passive evaporation, the observed enrichment is the result of the addition of the liquid−vapor IE and the fully expressed diffusive IE for compounds limited at the air-side boundary, or by the diffusive IE in the liquid phase in the case of liquid-limited compounds. (2) In air-flux evaporation, the same holds, but here, the air-side limited diffusive IE is reduced by airflow. (3) In low-pressure evaporation, the diffusive IE is reduced by the absence of air. In addition, low-pressure evaporation is very fast, which causes a fast advective downward movement of the liquid surface, which counteracts the creation of diffusion gradients in the liquid, and therefore only little diffusive fractionation occurs. (4) Distillation presents a more complex situation. In a distillation column, a liquid flows downward and a gas stream flows upward, creating a series of equilibrations in which isotopomer exchange between the liquid and the gas occur. The diffusive IE is fully suppressed since the liquid is in contact with saturated vapor. The temperature is usually near the boiling point of the distilled compound for practical purposes. Therefore, although the liquid−vapor IE is active, it is the IE for the boiling temperature, and not for ambient temperature. When the IE is normal, the liquid is enriched in the heavier isotope, and the bulk liquid in the flask becomes isotopically relatively enriched also. Condensed vapor taken at the top is therefore relatively depleted. Distillation has been used for measuring the liquid−vapor IE. As discussed before, the IE is highly dependent on the position of the isotope substitution, and it can therefore be expected that isotope enrichments during distillation are position-specific.

Bulk enrichment factors for distillation compared well with literature values (Supporting Information, Table S6), and were positive except for acetone, leading to vapors enriched in ^{13}C. This phenomenon was well recognized already in the classic literature and was explained based on the higher molar volume of compounds containing a ^{13}C, leading to higher vapor pressure.[30] Distillation of *n*-heptane (apolar) and toluene (weakly monopolar) did not reveal large PSIEs (Table 1). In contrast, for polar compounds, PSIEs are observed in DE and also in LPE experiments, probably due to the presence of stronger intermolecular interactions. In acetone, these bindings result in a lower volatility of ^{13}C isotopomers, thus in an overall normal IE in distillation, similar to the normal IE for ^{2}H and ^{18}O in water.

In our low-pressure evaporation experiments, IEs were small, but PSIEs were observable. This is a result of the liquid−vapor IE and a diminished diffusive IE. Boiling in the low-pressure evaporation leads to $h = 1$ conditions (eq 3), with suppressed diffusive IE.

In order to discuss the passive volatilization experiments, it must first be ascertained for which of these liquids the evaporation limitation lies on the air-side boundary. This was done using general concepts of mass transfer theory on liquid−gas boundaries (Supporting Information, Figure S2). The main criterion for separating liquids into either air-side limited, liquid-side limited or both-side limited liquids is the air−organic liquid partitioning coefficient K_{ial}. It is shown in Figure S2 that the transition from air-side limited to liquid-side limited evaporation is not sharp, and that there is a zone where both films may limit evaporation. Seven compounds in this study have, like water, a K_{ial} lower than 10^{-3}: methanol, ethanol, propan-1-ol, toluene, heptane, TAME and TCE. This means that for these only moderately volatile compounds, the air-side boundary limits passive evaporation, and eq 3 applies for explaining associated IEs. The evaporation of acetone seems to be limited equally by both sides (Figure S2). MTBE and bromoethane, the two most volatile compounds in this study, are limited rather more on the liquid side (Figure S2 and Table S4), and eq 4 applies for explaining the observed IEs.

In our passive evaporation experiments, bulk enrichments were reasonably well correlated with results from the literature (Table S6). For air-side limited liquids, passive evaporation is subject to two additive IE: the diffusive IE and the liquid−vapor IE (eq 1). Because our distillation experiments yielded enrichment factors for the vapor−liquid IE ($h = 1$ in eq 3), we can make use of eq 1 to obtain experimental diffusive IE via (eq 6)

$$IE\varepsilon_{diff-air} = IE_{PE} - \Delta_{liquid-vap} \quad (6)$$

According to our hypothesis, the experimental diffusive IE $\varepsilon_{diff\text{-}air}$ should not be position-specific. In Figure 3 we show the experimental diffusive IE $\varepsilon_{diff\text{-}air}$ for all compounds and all positions, obtained as (ε PE − ε DE) versus the bulk theoretically obtained $\varepsilon_{diff\text{-}air}$ from eq 3 with $n = 1$ (no airflow) and $h = 0$.

Figure 3 shows that for the liquids where passive evaporation is controlled on the air side, the observed effects are scattered but lie in the average near the prediction line, which represents no difference between the experimental and the theoretical diffusive IE values. The values for the two liquid-limited compounds and for acetone all lay above the prediction line. This means that experimental diffusive IEs are smaller than theoretical IEs in air, which comes from the fact that they are occurring in the liquid phase for these compounds. Acetone is the most illustrative in this context: for this small compound, a theoretical diffusive IE in air of −3.1‰ would be expected, but in our study, the effects were only −1.8‰ at C-1 or −2.3‰ at C-2. Bromoethane similarly showed a lower experimental IE than the predicted diffusive IE of −1.5‰, and, in addition, a very significant position-specific contribution: no IE at C-1 and

DOI: 10.1021/acs.est.5b03280
Environ. Sci. Technol. 2015, 49, 12782−12788

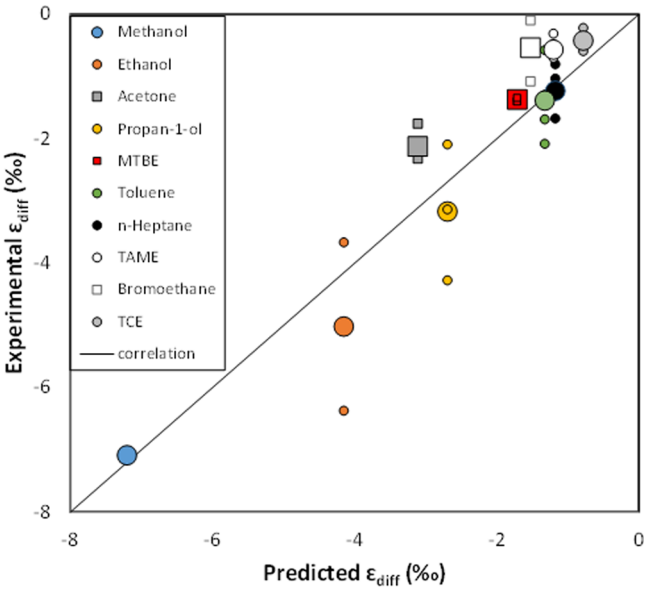

Figure 3. Calculated experimental diffusive IE values for bulk compound (large symbols) and each position (calculated as ε PE − ε DE, small symbols) versus theoretically predicted diffusive IE (Table S5, second column). Spheres represent liquids with air-side limitation, squares are liquid-side limited liquids. Black line is 1:1 slope.

−1.0‰ at C-2. This suggests that diffusive IEs created by liquid diffusion are position-specific because of interactions of the halogen in the liquid phase. MTBE was the only compound without any position-specific diffusive IE, but its bulk IE was also somewhat smaller than the one predicted by diffusion in air (Figure 3).

Passive evaporation of organic liquids limited by the air side boundary seems also to some extent to produce position-specific diffusive IEs. The most surprising is the strong enrichment of C-1 in ethanol (−6.1‰, instead of theoretical −4.1‰, Figure 3). In propanol, the diffusive IE is largest at the C-1 and smallest at the C-3, whereas at C-2, it is about equal to the theoretical value. A similar pattern is observed in toluene at C-1 and C-5 which are somewhat off the prediction line in Figure 3. However, as in propan-1-ol, the bulk mean fits very well that predicted by the CG-model and eq 3. In the most apolar compound *n*-heptane, the variation among positions spanning across ±0.50‰, is only slightly larger than the resolution limit of irm-^{13}C NMR (±0.2‰), and the bulk diffusive IE again fits very well that predicted by the CG-model and eq 3. For TCE, we find a smaller IE for C-1 of −0.2‰ compared to the predicted of −0.8‰. The vapor−liquid isotope effect of TCE was reported to depend quite strongly on temperature in the range of 5−50 °C,[9] and therefore, it may not be justified to compare this with our vapor−liquid IE from distillation. In contrast, toluene had a very constant vapor−liquid IE in the range of 5−70 °C.[10] For other compounds, temperature dependency is not known.[5]

The principal outcomes of this study are 2-fold. First, the study validates the CG-model for the interpretation of IEs during volatilization of organic liquids. For organic liquids where volatilization is controlled in the stagnant air boundary layer, it is established that the overall IE is the sum of the liquid−vapor IE and the diffusive IE in the air film. For liquids where the limitation is not clearly in the air film, lower diffusive IEs are observed. Thus, we both confirm and explain previous measurements of low diffusive IEs for TCE in water.[23] Second, we show that under both potential limiting regimes PSIEs are evidenced and that these can be in opposed directions, leading to bulk values that do not reflect the real fractionation occurring. Hence, we show that it is possible to create traceable changes in intramolecular isotope distributions in the remaining liquid.

Furthermore, we provide evidence that several other models for interpreting IEs during evaporation of liquids are not adequate for the interpretation of our data. For example, the model put forward in Figure 6 in the work of Harrington et al.[10] predicting depletion of C-isotopes in organic liquids during evaporation is not supported because we find enrichment of remaining liquids in all cases except TCE. Also, the equation for theoretical isotope fractionation given by Xiao et al.[17] (eq 6 in their work) does not give any quantitative explanation of the evaporation phenomenon; indeed, it overestimates the diffusive fractionation by a factor of 2−3. The model given by Jeannottat and Hunkeler,[14] derived from the He and Smith[3] model, is closest to our experimental observations. That model, which takes into account fractionation as a function of the rate of volatilization for TCE, introduces two end points: at an infinitely low rate of volatilization, it predicts that the IE is fully developed as a sum of liquid−vapor IE plus diffusive IE, whereas at a high rate of volatilization the effects would tend to disappear and no isotope fractionation would occur. However, for a quantitative application of that model, the thickness of the liquid diffusive boundary layer has to be known, which is in practice very difficult. Further work should look also at the influence of stirring the liquid phase and better explain why alcohols in passive evaporation undergo an unexpectedly high normal isotope effect at the C-1 position, that bearing the hydroxyl group.

■ ASSOCIATED CONTENT

Supporting Information

The Supporting Information is available free of charge on the ACS Publications website at DOI: 10.1021/acs.est.5b03280.

More detailed data on materials and analytical methods, characteristics of compounds, comparison of bulk isotope enrichment factors with literature values, and method for calculating enrichment factors. (PDF)

■ AUTHOR INFORMATION

Corresponding Author

*Phone: +33 4 13 55 10 34. Fax +33 4 13 55 10 60. E-mail: patrick.hohener@univ-amu.fr.

Notes

The authors declare no competing financial interest.

■ ACKNOWLEDGMENTS

This work is funded by the French National Research Agency ANR, project ISOTO-POL funded by the program CESA (no. 009 01). M.J. thanks the ANR for funding his PhD bursary through this project. We thank Ms. Anne-Marie Schiphorst for help with irm-MS measurements.

■ REFERENCES

(1) Elsner, M. Stable isotope fractionation to investigate natural transformation mechanisms of organic contaminants: principles, prospects and limitations. *J. Environ. Monit.* **2010**, *12*, 2005−31.

(2) Craig, H.; Gordon, L. I. Deuterium and Oxygen-18 Variations in the Ocean and the Marine Atmosphere. In *Conference on Stable Isotopes*

DOI: 10.1021/acs.est.5b03280
Environ. Sci. Technol. 2015, 49, 12782−12788

in Oceanographic Studies and Paleotemperatures; Tongiorgi, E., Ed. Spoleto, Italy, 1965; p 9.
(3) He, H.; Smith, R. B. An advective-diffusive isotopic evaporation-condensation model. *J. Geophys. Res.* **1999**, *104*, 18619−30.
(4) Mook, W. G.; De Vries, J. J. *Environmental Isotopes in the Hydrological Cycle: Principles and Applications, VOL. I: Introduction - Theory, Methods, Review*; IAEA, Isotope Hydrology Section: Vienna, 2000.
(5) Jancso, G.; Van Hook, W. A. Condensed Phase Isotope Effects (Especially Vapor Pressure Isotope Effects). *Chem. Rev.* **1974**, *74*, 689−750.
(6) Baertschi, P.; Kuhn, W.; Kuhn, H. Fractionation of isotopes by distillation of some organic substances. *Nature* **1953**, *171*, 1018−20.
(7) Narten, A.; Kuhn, W. Der $^{13}C/^{12}C$-Isotopieeffekt in Tetrachlorkohlenstoff und in Benzol. *Helv. Chim. Acta* **1961**, *44*, 1474.
(8) Balabane, M.; Letolle, R. Inverse overall isotope fractionation effect through distillation of some aromatic-molecules (Anethole, Benzene and Toluene). *Chem. Geol.* **1985**, *52*, 391−96.
(9) Poulson, S. R.; Drever, J. I. Stable isotope (C, Cl, and H) fractionation during vaporization of trichloroethylene. *Environ. Sci. Technol.* **1999**, *33*, 3689−94.
(10) Harrington, R. R.; Poulson, S. R.; Drever, J. I.; Colberg, P. J. S.; Kelly, E. F. Carbon isotope systematics of monoaromatic hydrocarbons: vaporization and adsorption experiments. *Org. Geochem.* **1999**, *30*, 765−75.
(11) Bouchard, D.; Hunkeler, D.; Gaganis, P.; Aravena, R.; Höhener, P.; Kjeldsen, P.; Broholm, M. M. Carbon isotope fractionation during migration of petroleum hydrocarbon vapors in the unsaturated zone: field experiment at Værløse Airbase, Denmark, and modeling. *Environ. Sci. Technol.* **2008**, *42*, 596−601.
(12) Bouchard, D.; Höhener, P.; Hunkeler, D. Carbon isotope fractionation during volatilization of petroleum hydrocarbons and diffusion across a porous medium: a column experiment. *Environ. Sci. Technol.* **2008**, *42*, 7801−06.
(13) Kuder, T.; Philp, P.; Allen, J. Effects of volatilization on carbon and hydrogen isotope ratios of MTBE. *Environ. Sci. Technol.* **2009**, *43*, 1763−68.
(14) Jeannottat, S.; Hunkeler, D. Chlorine and carbon isotopes fractionation during volatilization and diffusive transport of trichloroethene in the unsaturated zone. *Environ. Sci. Technol.* **2012**, *46*, 3169−76.
(15) Huang, L.; Sturchio, N. C.; Abrajano, T.; Heraty, L. J.; Holt, B. D. Carbon and chlorine isotope fractionation of chlorinated aliphatic hydrocarbons by evaporation. *Org. Geochem.* **1999**, *30*, 777−85.
(16) Shin, W. J.; Lee, K. S. Carbon isotope fractionation of benzene and toluene by progressive evaporation. *Rapid Commun. Mass Spectrom.* **2010**, *24*, 1636−40.
(17) Xiao, Q. L.; Sun, Y. G.; Zhang, Y. D.; Chai, P. X. Stable carbon isotope fractionation of individual light hydrocarbons in the C-6-C-8 range in crude oil as induced by natural evaporation: Experimental results and geological implications. *Org. Geochem.* **2012**, *50*, 44−56.
(18) Julien, M.; Parinet, J.; Nun, P.; Bayle, K.; Höhener, P.; Robins, R. J.; Remaud, G. S. Fractionation in position-specific isotope composition during vaporization of environmental pollutants measured with isotope ratio monitoring by ^{13}C nuclear magnetic resonance spectrometry. *Environ. Pollut.* **2015**, *205*, 299−306.
(19) Schwarzenbach, R. P.; Gschwend, P. M.; Imboden, D. M. *Environmental Organic Chemistry*, 2nd ed., Chapter 20; Wiley: Hoboken, NJ, 2003.
(20) Geiseler, G.; Fruwert, J.; Huttig, R. Dampfdruck- und Schwingungsverhalten der Stellungsisomeren n-Octanole und hydroxydeuterierten n-Octanole. *Chem. Ber.* **1966**, *99*, 1594−1601.
(21) Botosoa, E. P.; Caytan, E.; Silvestre, V.; Robins, R. J.; Akoka, S.; Remaud, G. S. Unexpected fractionation in site-specific C-13 isotopic distribution detected by quantitative C-13 NMR at natural abundance. *J. Am. Chem. Soc.* **2008**, *130*, 414−415.
(22) Craig, H. The geochemistry of stable carbon isotopes. *Geochim. Cosmochim. Acta* **1953**, *3*, 53−92.
(23) Van Breukelen, B. M.; Rolle, M. Transverse hydrodynamic dispersion effects on isotope signals in groundwater chlorinated solvents' plumes. *Environ. Sci. Technol.* **2012**, *46*, 7700−08.
(24) LaBolle, E. M.; Fogg, G. E.; Eweis, J. B.; Gravner, J.; Leaist, D. G. Isotopic fractionation by diffusion in groundwater. *Water Resour. Res.* **2008**, *44*, W07405.
(25) Wanner, P.; Hunkeler, D. Carbon and chlorine isotopologue fractionation of chlorinated hydrocarbons during diffusion in water and low permeability sediments. *Geochim. Cosmochim. Acta* **2015**, *157*, 198−212.
(26) Bourg, I. C.; Sposito, G. Isotopic fractionation of noble gases by diffusion in liquid water: Molecular dynamics simulations and hydrologic applications. *Geochim. Cosmochim. Acta* **2008**, *72*, 2237−47.
(27) Silvestre, V.; Mboula, V. M.; Jouitteau, C.; Akoka, S.; Robins, R. J.; Remaud, G. S. Isotopic ^{13}C NMR spectrometry to assess counterfeiting of active pharmaceutical ingredients: Site-specific ^{13}C content of aspirin and paracetamol. *J. Pharm. Biomed. Anal.* **2009**, *50*, 336−41.
(28) Bayle, K.; Akoka, S.; Remaud, G. S.; Robins, R. J. Nonstatistical ^{13}C distribution during carbon transfer from glucose to ethanol during fermentation is determined by the catabolic pathway exploited. *J. Biol. Chem.* **2015**, *290*, 4118−4128.
(29) *Evaluation of Measurement Data—Guide to the Expression of Uncertainty in Measurement*, JCGM 100:2008; Joint Committee for Guides in Metrology, 2008
(30) Bartell, L. S.; Roskos, R. R. Isotope effects on molar volume and surface tension - simple theoretical model and experimental data for hydrocarbons. *J. Chem. Phys.* **1966**, *44*, 457−463.

DOI: 10.1021/acs.est.5b03280
Environ. Sci. Technol. 2015, 49, 12782−12788